CONF-9010212--20

BNL--45296

DE91 004007

OG 1125
Subm. to Symposium on Detector Research and Development
for the SSC, Fort Worth, TX, Oct. 15-18, 1990

SILICON DRIFT DEVICES FOR TRACK AND VERTEX DETECTION AT THE SSC

W. Chen, H. Kraner, Z. Li, C. Ng, V. Radeka, P. Rehak, S. Rescia
Brookhaven National Laboratory, Upton NY 11973

J. Clark, S. Henderson, L. Hsu, J. Oliver, R. Wilson
Harvard University, Cambridge, MA 02138

M. Clemen, T. Humanic, D. Kraus, G. Vilkelis, B. Yu
University of Pittsburgh, Pittsburgh, PA 15260

K. McDonald, C. Lu, M. Wall
Princeton University, Princeton, NJ 08544

A. Vacchi
Rockefeller University, New York, NY 10021

G. Bertuccio, E. Gatti, A. Longoni, M. Sampietro
Politecnico di Milano, Piazza Leonardo da Vinci 32, Milano

P. Holl, L. Strüder
Max-Planck-Institut for Extraterrestrial Physics, D–8046 Garching

E. Lorenz
Max-Planck-Institut for Physics, D–8000 Munich 40

U. Faschingbauer, A. Wörner, P. Wurm
Max-Planck-Institut for Nuclear Physics, D–6900 Heidelberg 1

J. Kemmer
Technische Universität München, D–8046 Garching

Received by OSTI

NOV 2 3 1990

DISCLAIMER

This report was prepared as an account of work sponsored by an agency of the United States Government. Neither the United States Government nor any agency thereof, nor any of their employees, makes any warranty, express or implied, or assumes any legal liability or responsibility for the accuracy, completeness, or usefulness of any information, apparatus, product, or process disclosed, or represents that its use would not infringe privately owned rights. Reference herein to any specific commercial product, process, or service by trade name, trademark, manufacturer, or otherwise does not necessarily constitute or imply its endorsement, recommendation, or favoring by the United States Government or any agency thereof. The views and opinions of authors expressed herein do not necessarily state or reflect those of the United States Government or any agency thereof.

Abstract

We report on the recent progress in the study of Semiconductor Drift (Memory) Detectors intended for an inner tracking and vertexing system for the SSC. The systematic studies and the calibration of the existing detectors and the simulated performance in the actual SSC environment are highlighted.

Introduction

This collaboration is committed to develop a vertex and an inner tracking detector for the SSC based on Semiconductor Drift (Memory) Detectors. We believe that silicon drift detectors are ideal detector elements to be used for the charged particle tracking close to the interaction region of the SSC for the following reasons:

1. the unambiguous position resolution of only several μm in two perpendicular directions
2. attribution of hits belonging to different bunch crossings with a timing accuracy better than $1ns$ and
3. the intrinsic signal pipeline within the very volume of the silicon drift detector.

This contribution is organized as follows. It starts with a brief description of silicon drift detectors, followed by an analysis of rate capabilities of silicon drift detectors in the SSC environment. The main part of the contribution describes the systematic studies done on a multi-anode detector. The next section reports on the Monte Carlo simulation of the silicon drift detectors performance in the SSC environment. A short list of conclusions closes this contribution.

Semiconductor Drift Detectors - Description

Silicon drift detectors are a relatively new kind of semiconductor detector able to provide very precise position and ionization measurements with a very modest

DISTRIBUTION OF THIS DOCUMENT IS UNLIMITED

MASTER

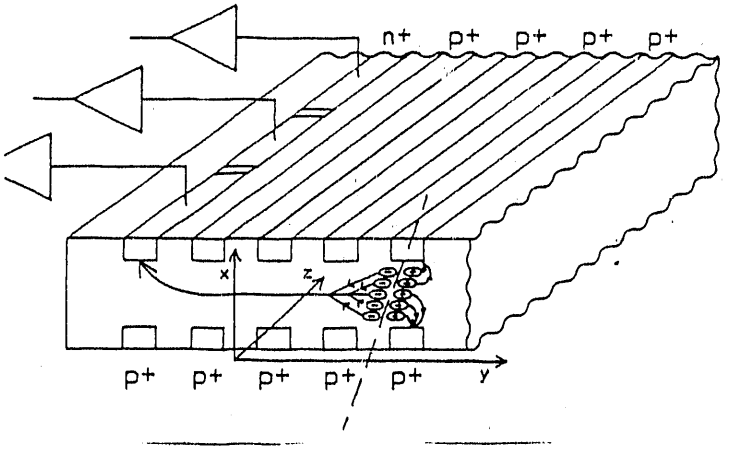

Figure 1: Perspective view (not to scale) of a semiconductor drift detector. Electrons created by an ionizing particle are transported long distances parallel to the detector surface. The anode is divided into short segments to measure the coordinate perpendicular to the drift direction.

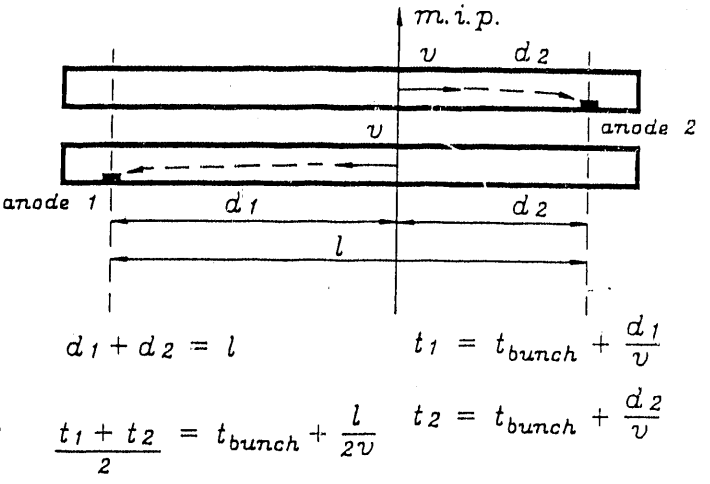

Figure 2: View (not to scale) of two silicon drift detectors placed in such a way that a particle crosses both detectors and the produced electrons drift in opposite directions with the same speed v. The sum of drift distances for any position of the incident particle is constant and equals the distance between anode 1 and anode 2. The average of two arrival times gives the time of the bunch crossing.

amount of electronics. A perspective view of the drift detector[1] is shown in Fig. 1. In principle, the electric field of thedrift detector forces electrons liberated by an ionizing particle to drift parallel to the large semiconductor surface to the anode. The transit time of electrons inside the detector measures the distance of an incident particle from the anode.

As a direct consequence of this electron transport method, the anode capacitance is much lower than that of a classical semiconductor detector of the same dimensions. The amplifier noise can be made much smaller, which is the main reason behind the excellent position resolution obtained from silicon drift detectors.

The measured position resolution in a test beam was $10\mu m$ over a drift distance of $4000\mu m$. These results[2] were achieved in fact with external amplifiers which were not matched to the very low anode capacitance.

We would like to stress that the maximum drift time is not the dead time of the silicon drift detectors. Due to the fact that all electrons are continuously drained at the anode, silicon drift detectors have no dead time. Electrons drifting toward the anode have their charges screened by the electrode structure of the silicon drift detector and do not interfere with the other signals or with the signal processing at the anode.

Fig. 1 shows the collection anode divided into individual pad-anodes. The position of the responding anode(s) measures the coordinate perpendicular to the drift direction. Due to the transverse diffusion, the electrons produced by the ionization arrive as a gaussian shaped charge cloud in the anode region. Ordinarily, charge will be collected on more than one anode. The charge division method yields the position of the crossing particle in the second coordinate with a precision of about 4% of the anode pitch. Thus, a multi-anode silicon drift detector provides unambiguous two dimensional position information. The position information is similar to that which is expected from proposed silicon pixel devices. The multi-anode silicon drift detector provides better resolution with four orders of magnitude fewer read-out channels.

Rate Capabilities of Silicon Drift Detectors

In the high rate environment of the SSC a silicon drift detector stores at any given time hits of particles originated at different bunch crossings. Fig. 2 shows a simple method to time hits in a silicon drift detector. Two silicon drift detectors are placed parallel one to another at a small distance.The drift fields in the two detectors are arranged in such a way that electrons drift in opposite directions in these two detectors. Following a simple calculation described in Fig. 2, we see that there is a constraint for the sum of the drift times measured in both detectors with respect to the time of the particle crossing. The time resolution of each drift detector is better than $1ns$. The mean value of the drift times of the pair of drift detectors and hence the bunch crossing timing can be determined with a resolution better than $1ns$. We see that we have no problem with the bunch crossing association in the case of a single particle within

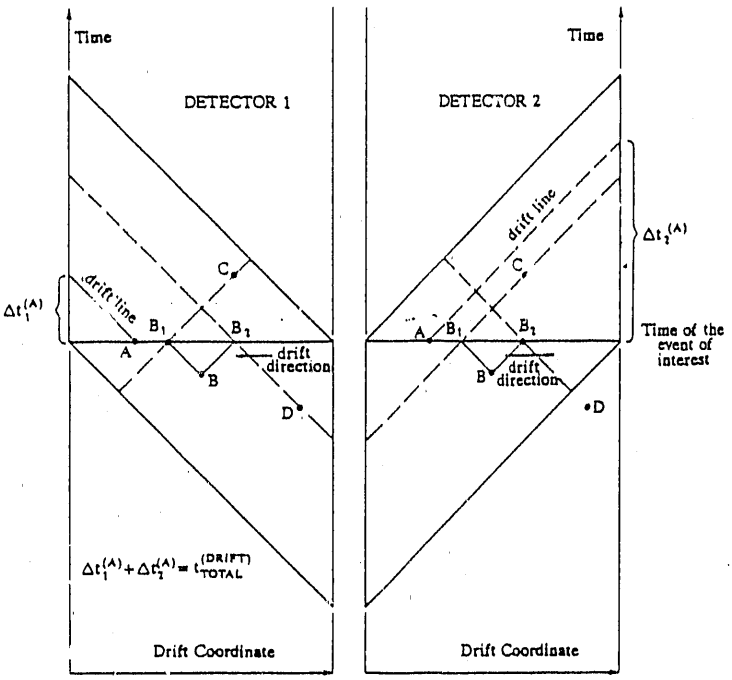

Figure 3: The drift of electrons in a silicon drift detector can be visualized by drift lines on a space–time plot. The drift coordinate is the horizontal axis, and the time is the vertical axis. The two diagrams represent the two parallel detectors drifting electrons in opposite directions.

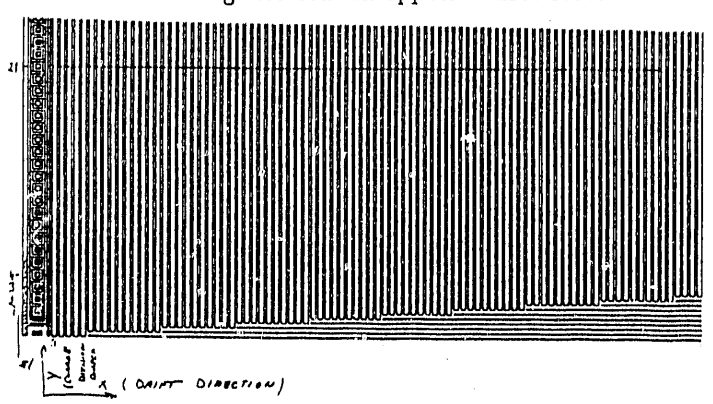

Figure 4: P^+ mask of an existing 41 anode drift detector

an anode and memory time of the detector. In the case of several particles produced at different bunch crossings and detected at the anode during the memory time of the silicon drift detector the analysis is more complicated.

In Fig. 3 we see a diagram visualizing the drift of electrons in a space–time plot. The vertical axis represent the time, the horizontal axis the drift distance. Hits on the detector originating within the same beam crossing are distributed along a horizontal line. As they drift, they move upwards along diagonal lines called drift lines until intersecting the vertical axis. The drift line of each detector points in the electron drift direction.

One can see from this diagram that there is a minimum time over which digitization must be recorded to acquire all information for a given beam crossing time. Within this minimum time, there is still a large area in the space–time from which hits are being collected. Hits early enough in time, far enough from the anodes, would be near the bottom of this diagram. The space–time area enclosed within the thick lines in Fig. 3 is mapped onto the one–dimensional vertical time axis.

The method of identifying hits produced at the time of the event of interest is the method displayed in Fig. 2. Hit "A", for instance, will drift in detector 1 diagonally up and to the left until intersecting the vertical axis approximately at 1/4 of the total drift time. In detector 2, this intersection is approximately at 3/4 of the total drift time. The sum is simply the total drift time. Hits occurring out of time will add to some other value.

In the case of several hits, with the projection onto the time of interest there is the possibility that an incorrect pairing of two hits out of time in two detectors will mimic a hit in time of interest. Let us consider the hit "B" in Fig. 3. The intersection of the drift line of hit B in detector 1 (2) with the time of the event line is called B_1 (B_2). Hits B and B_1 are projected onto the same point on the time axis of detector 1. Hit "C" in Fig. 3 was placed on the drift line of detector 2 passing through the point B_1. Again, hits C and B_1 are projected onto the same point on the time axis of detector 2. In the described case hit B in detector 1 can be paired with the hit C in detector 2 to produce an in time phantom hit called B_1. Similarly, in Fig. 3 there is a construction of the symmetrical phantom hit. The hit B in detector 2 can be paired with the hit D in detector 1 to produce a phantom hit called B_2.

The probability for an out of time hit B to produce an in time phantom hit after being incorrectly paired with the other hit C from a uniformly populated space–time area is $\simeq 2 \times \delta t / t_{total}^{drift}$ where δt is a combined time accuracy of the drift detector (2ns) and t_{total}^{drift} is the maximum drift time (2 μs). This probability in the case of a single pair is about 0.2%. In the case of n out of time hits the probability of a phantom in time hit would be n^2 times larger.

We can see that silicon drift detectors can operate in rates producing up to 2–4 out of time hits per anode, within the memory time of the detector without compromising the performance. We may take advantage of the multiple hit capability to decrease the amount of electronics associated with the silicon drift detector tracking system.

Systematic Studies of Silicon Drift Detectors

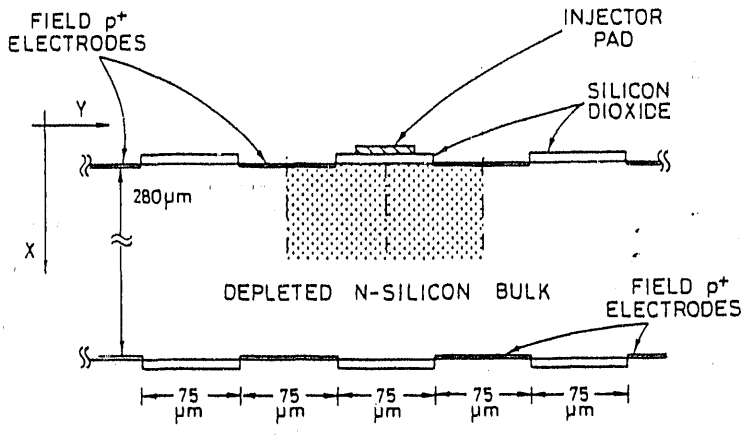

Figure 5: Cross section of the Silicon drift detector in the injector region. The z-direction is perpendicular to the plane.

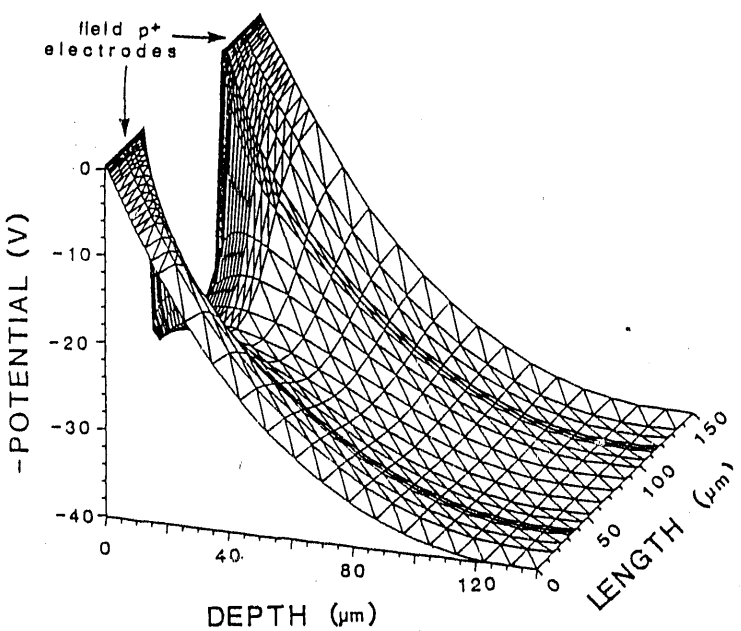

Figure 6: Potential energy for electrons calculated within the dotted area on the previous Figure.

Experimental apparatus

Most of the measurements presented in this section were performed with a multi-anode (41) linear drift detector, shown in Fig. 4. This is a rectangular detector made of $300\mu m$ thick 10 $k\Omega cm$ NTD n-type silicon. The detector is 1.5 cm long in the drift direction and 1 cm wide. The lateral resolution is obtained by charge sharing between 41 anodes, spaced 250 μm apart. There is an implanted voltage divider directly on the detector, located right at the center, above anode No. 21. The detector was manufactured in 1984 at TU Munich and tested at the SPS beam at CERN.[2]

To simulate the ionization produced by a minimum ionizing particle, infrared light pulses were used. A GaAs laser diode was the source of light pulses, having duration of a few ns at a wavelength of about 900nm. Light pulses were carried in a $100\mu m$ diameter fiber and focused onto the detector surface by microscope optics. The spot size was demagnified down to a $5\mu m$ diameter spot. The detector assembly was mounted on an x-y stage movable by stepping motors and controlled by a PC. The mechanical precision was $2-3\mu m$ with about the same degree of reproducibility. To measure the temperature of the silicon drift detector a platinum thin film temperature sensitive resistor was glued onto a corner of the detector. Although the temperature could be read within 0.1K, the temperature of the sensor might not correspond precisely to the detector temperature. All the equipment was bought with funds from the SSC R&D program.

Temperature Dependence of the Drift Velocity and its Calibration

The silicon drift detectors are quite sensitive to temperature changes. The drift velocity in silicon depends on the absolute temperature as $T^{-2.4}$. Due to the precision of the drift coordinate measurement, silicon drift detectors are sensitive to temperature variations of about 0.1K. Stabilizing the overall temperature to better than 0.1K may not be practical. Rather, it seems easier to calibrate the drift velocity.

A practical calibration of the drift velocity must be accomplished by simple and reproducible means, ideally by pulsing an electrode at a given distance from the anode.[3] Such an injecting electrode was implemented on a silicon drift detector to be used in the UA6 experiment at the CERN SPPS.[4] The injector is a small metallic gate deposited on the silicon dioxide present between the field p^+ strips, at the desired position. A cross section of the detector around an injector pad is shown in Fig. 5. The injector is a metal on silicon (MOS) capacitor. The injection mechanism is related to the actual shape of the potential energy for electrons in a silicon drift detector with working biases. The shape of the potential energy for electrons is shown in Fig. 6 for the dotted region of Fig. 5.

The positive charge at the $Si-SiO_2$ interface causes a downward bending of the potential at the interface. There are many electrons confined in the surface region extending up to the saddle point. The number of accumulated electrons in this surface region is the maximum that the region can hold. An additional electron falling into this region would deform the potential energy upward and one electron would escape into the main valley of the detector. (This dynamic equilibrium was used by the program to calculate the potential within the detector shown in Fig. 6.)

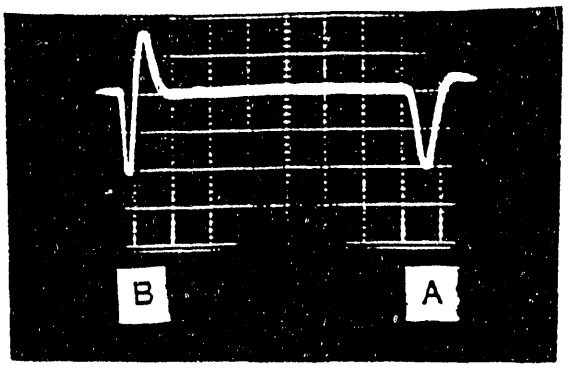

Figure 7: A–pulse corresponding to the collection of the injected charge after an electron drift time of $3.8\mu s$. B–injection start pulse.

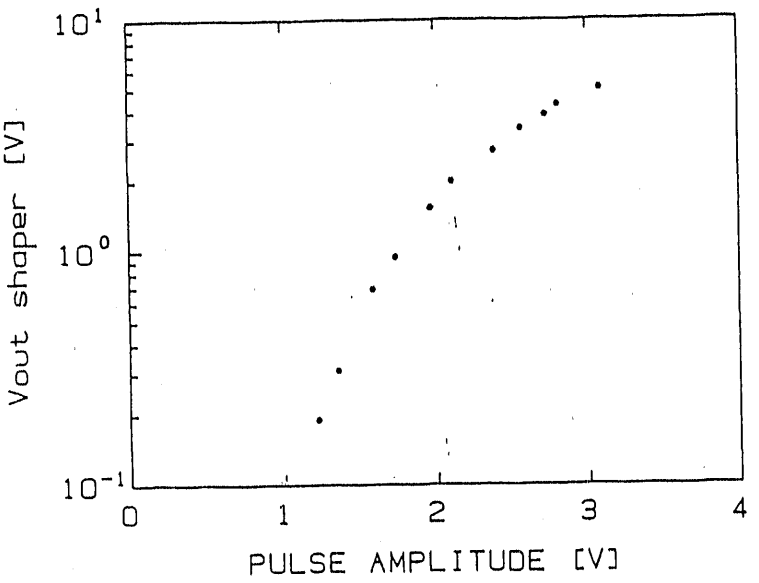

Figure 8: Injected charge as a function of the amplitude of the voltage pulse applied to the injector electrode. Note the log scale for the injected charge.

Accumulated electrons are candidates for being injected into the main valley of the detector. Let us assume some negative charge is brought on the metallic gate covering the SiO_2, by applying a negative voltage pulse to the gate. A portion of the positive charges is neutralized and electrons from the surface region are pushed above the saddle point into the main valley. After the injection and the return of the gate potential to the original value, the electrons are replenished from the path along the z–direction. Thus, the pulse repetition rate may approach 0.5Mhz in the detector, without appreciable rate dependent effects.

We have implemented and tested injectors at a distance of about 2cm from the anode. The size of the metal gate was $45 \times 125\mu m^2$. The drift field was 492

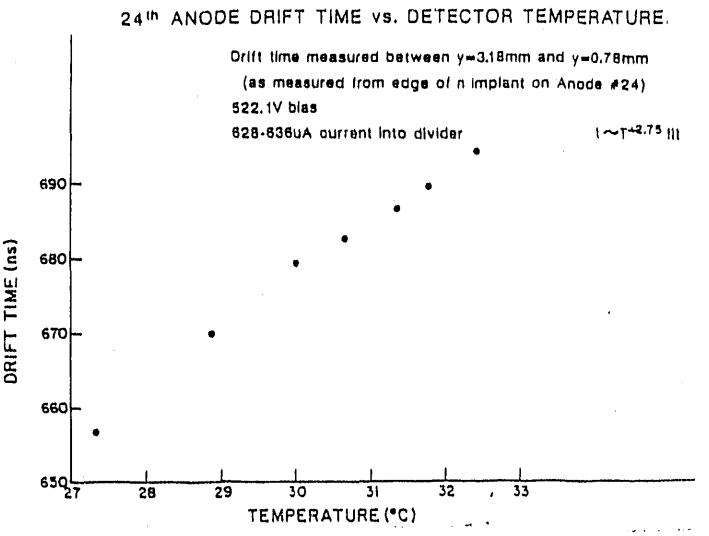

Figure 9: Drift time for 2.4mm drift distance as a function of the detector temperature.

V/cm corresponding to an electron drift time of $3.8\mu s$. Fig. 7 shows the waveform of the pulse–shaped anode signal. Pulse A corresponds to about 25000 electrons, equivalent to the charge liberated by the passage of a minimum ionizing particle through the detector. Pulse B is the prompt pulser signal applied to the p^+ electrode surrounding the collecting anode.

Fig. 8 shows the dependence of the injected charge on the amplitude of the pulse applied to the electrode. For small pulses, the linear part (on a semilogarithmic scale) of the curve has a slope smaller by a factor of 10 than that of an ideal junction diode. We believe we understand the behavior. For the detector calibration Fig. 8 shows that charges up to several times the charge liberated by a minimum ionizing particle can be injected into the detector.

The tested injection scheme is not the only one considered by the collaboration. We have a different injection scheme for the drift velocity calibration in the existing, but not yet tested cylindrical silicon drift detector. We are studying a third calibration scheme for the Mark–1 SSC silicon drift detector.

The dependence of the drift time on the temperature of the detector was measured in the 41 anode detector described at the beginning of this section. Fig. 9 shows the dependence of the drift time on the temperature. The drift field was 278V/cm and the net drift distance 2.4 mm. The best fit gives the drift time to be proportional to the 2.75 power of the absolute temperature. Removing one extreme point from the sets of measurements the power decreases to 2.5, which is in reasonable agreement with the published value of 2.42, knowing that the measured temperature is not necessarily the detector temperature.

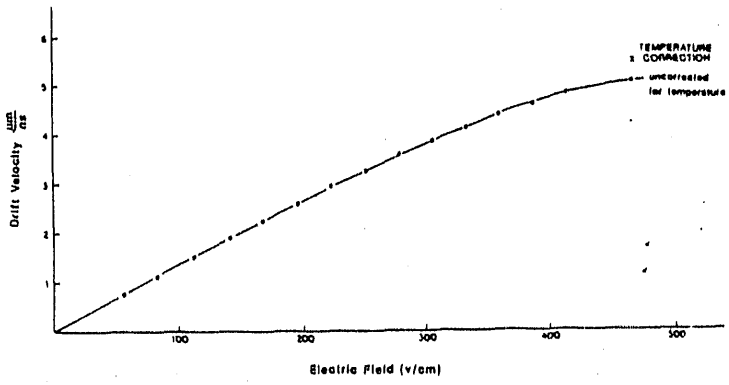

Figure 10: Drift velocity in a hyperpure silicon detector as a function of the drift field at the detector temperature. Correction corresponds to 300K.

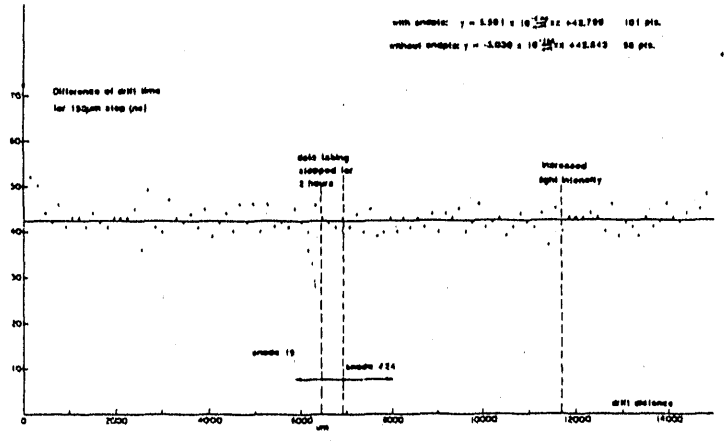

Figure 11: Differences of drift time for $150\mu m$ steps along the drift direction.

At this point it is important to comment briefly on the dependence of the drift velocity on the drift field. There should be a simple linear dependence with the constant of proportionality known as the electron mobility. Fig. 10 shows the measured dependence. The measurement was performed for most of the points at 300K. At higher drift fields heating of the detector due to the power dissipated in the voltage divider was observed. The cross indicates the amount of the temperature correction. There are two important consequences of the curve shown on Fig. 10:

1. The mobility is lower than the published value already at the lower portion of the curve ($1330 cm^2/Vs$ as compared to $1500 cm^2/Vs$).
2. We see a small saturation effect for the drift fields as low as 200V/cm.

The saturation of the drift velocity is a mixed blessing for the performance of silicon drift detectors. Although the ideal isochronism is compromised, the stability is improved and the effects of the external magnetic field are reduced.

Differential non–linearities in the position measurement along the drift coordinate

A very careful measurement of the dependence of the drift time on the drift distance was performed. The position of the detector was repeatedly moved one period of the drift electrode structure, that is, $150\mu m$. The drift field was 278V/cm and the temperature 300K. The drift time was read on the scope as the edge of a zero crossing discriminator output which followed a differentiated pseudo–gaussian shaping amplifier. We did not have a TAC with suitable dynamic range for the measurement.

The integral linearity line is too straight to indicate any deviation and is not shown. Fig. 11 shows the differential non–linearity, that is, the plot of differences of the drift time measurements for each $150\mu m$ step. All points are scattered about the fitted line which shows a slope very near zero. The constant value of the time difference indicates that the drift velocity is constant along the drift direction for the detector under study. There are a few higher points at the short drift distances and one much higher point at the end of the drift region. The non–linearity at the small values of the drift distances is due to a non–ideal drift field in the anode region which penetrates into the periodic region of the detector. The voltage in the anode region can be adjusted to remove this non–uniformity, or a correction can be applied later in the off–line analyses. The non–linearity at the end of the detector cannot be corrected in hardware and a software correction is required.

The measurement of differential non–linearities plotted in Fig. 12 shows an interesting structure. The measurement is similar to the previous one, however, the step was decreased to $50\mu m$ and only the first 4mm of the detector was scanned. At the left side of the plot we can see again the penetration of the electric field from the anode region. The most striking feature is the appearance of 3 bands into which all measured points fall. Moreover, there is a periodicity of 3 measurements corresponding to the $150\mu m$ pitch of the detector drift structure. The drift time measurement corresponding to the second position difference is longer than the third one and the first time interval is the shortest of all. An explanation of the structure is shown on the upper right corner of Fig. 12, where the periodic structure of the detector together with the light injection points are shown.

The electric field close to the detector surface does not have a constant component along the drift direction as is the case in an ideal detector or the central part of the detector under study. The drift field is zero right at the

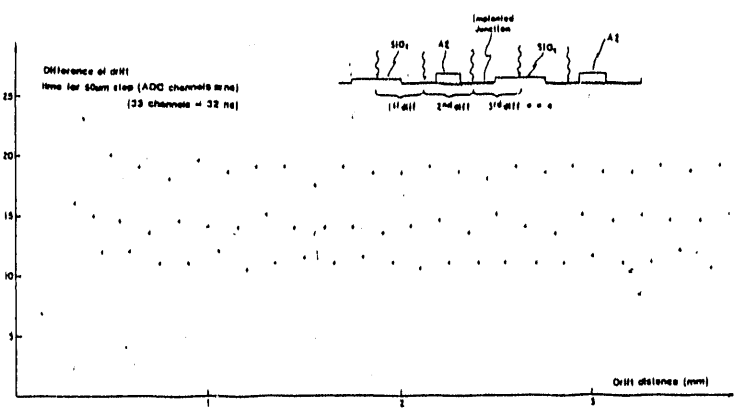

Figure 12: Drift time differences for $50\mu m$ steps along the drift direction.

rectifying junction and 3 times stronger than the average field at the $Si - SiO_2$ interface. There is, however, a large difference in the location across the thickness of the detector of the charge liberated by our laser light and by an ionizing particle. The absorption length of 900nm light in silicon is about $20\mu m$, whereas a fast particle produces electron-hole pairs uniformly across the detector thickness. The drift time differences are therefore amplified with the light test. The analysis of the effect for minimum ionizing particles is published in Ref. 2. The error is about $5\mu m$ when no correction for the effect as a function of the drift coordinate is applied, and can be reduced to $2\mu m$ with a fine correction equivalent to a non-constant drift velocity. The effect cannot be completely corrected due to the fluctuations of the density of the ionization of a fast particle crossing the detector.

Independence of the drift time on the coordinate transverse to the drift direction

In an ideal drift detector the drift time is independent of the transverse coordinate. In a multi-anode detector there is one constant per anode which takes into account slightly different delays of the signal cable, differences in the signal processing electronics, etc. There may be other imperfections within the detector which may require individual calibration of anodes and in an extreme case, a complicated correction may be required. The most obvious imperfection is the non-uniformity of the silicon doping which deforms the drift trajectories and changes the local drift velocity.

Fig. 13 shows the drift time measured on several anodes for drift distances ranging from 0.3 to 5.7mm. The drift field was 335V/cm. A more detailed analysis of the data shown in Fig. 13 indicates that the drift velocities for anodes in the center of the detector are slightly lower than the drift velocity closer to the detector sides. This difference can be attributed to the higher temperature of the detector in the center due to the presence of the

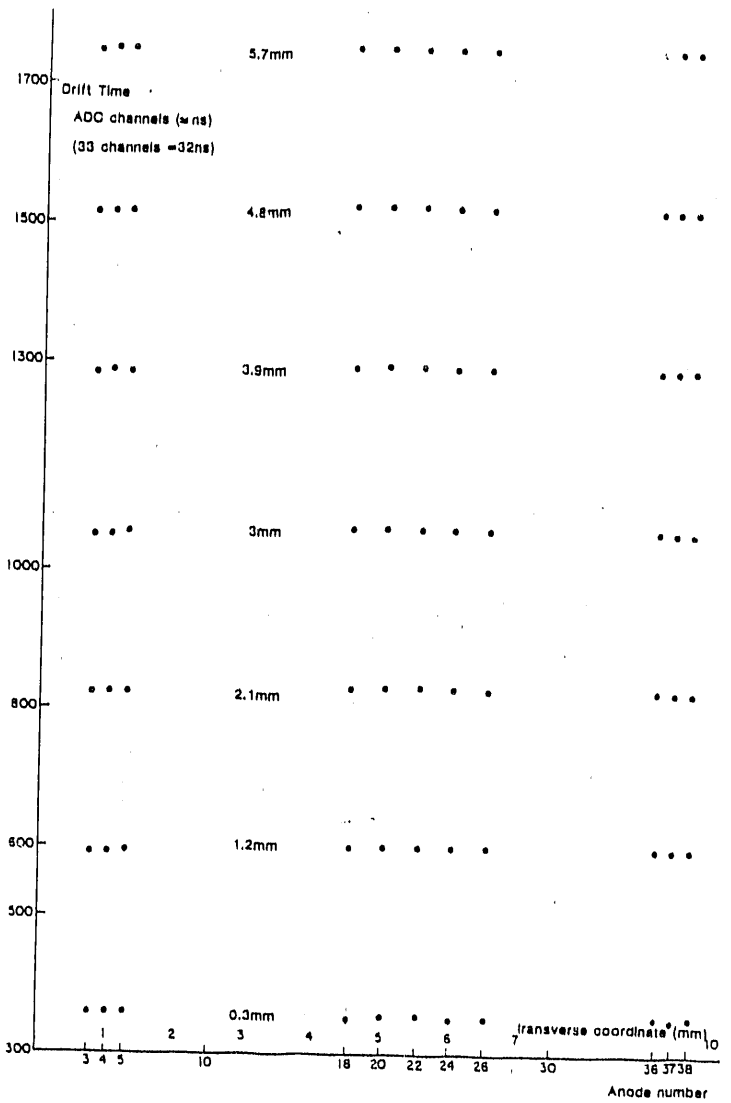

Figure 13: Drift time as a function of the transverse coordinate for several drift distances.

voltage divider implanted directly on the center of the detector.

The uniformity of the drift coordinate measurement after the adjustment of the first measured delay (at 0.3mm) to the same value, and removing the temperature dependence, was about $6\mu m$.

It is obvious that a correctly designed silicon drift detector should have a uniform temperature when properly biased. The voltage divider must not cause temperature gradients within the detector.

Independence of the transverse coordinate measurement on the drift coordinate

This is a complementary study relative to the study of the previous subsection. Multi-anode silicon drift detectors measure the transverse coordinate by the charge division among anodes where the diffused charge is collected. Interpolation among anodes leads to an increase

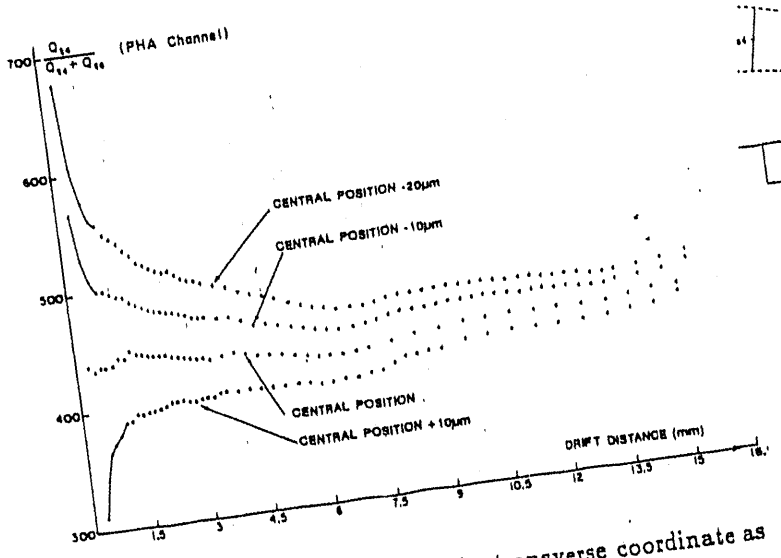

Figure 14: Measurement of the transverse coordinate as a function of the drift distance.

in the precision of the measurement of the transverse coordinate to as low as several percent of the inter–anode spacing. This measurement assumes that the signal electrons drift on straight lines perpendicular to the field defining electrodes of the detector. Doping non–uniformities of the silicon may distort drift trajectories and interfere with the measurement of the transverse coordinate.

Fig. 14 shows the ratio of the charge collected at anode 24 divided by the sum of charges collected at anodes 24 and 25 versus the drift distance. The light spot was positioned close to the middle position between the two anodes. For shorter drift distances where the charge diffuses only to these two anodes the measured ratio is a very sensitive function of the position. For longer distances the charge spreads among more anodes and the sensitivity of the ratio to the transverse position is decreased. The plotted ratio is not the best method of measuring the transverse coordinate for longer drift distances. At the time of measurement we did not have a read–out system capable of reading more than one ADC channel and calculating the centroid of the charge.

Fig. 14 shows the four series of measurements, each series taken with the position of the spot moved by $10\mu m$ in the transverse direction. If we attribute all deviations from the perfect lines to the imperfection of the detector (there may be a systematic error due to the DC offset of one of the linear amplifiers used during the measurement) than the systematic error in the measurement of the transverse coordinate is about $10\mu m$. The error can be decreased to $4\mu m$ by calibrating out the linear part of the systematic deviations.

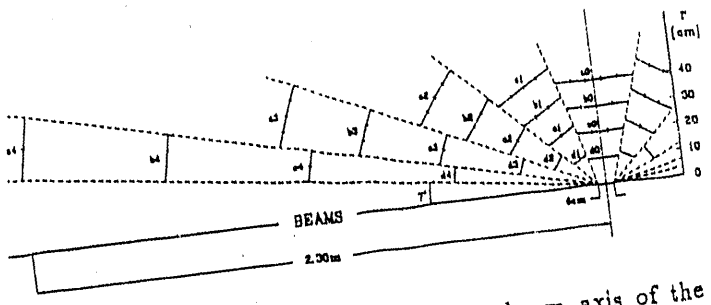

Figure 15: Cross section along the beam axis of the inner tracking detector based on silicon drift detectors. Detector has a full azimuthal coverage and rapidity coverage $|\eta| \leq 3$. Lines indicate the cross section of rings of detectors centered around the beam axis. Each line represents close layers of silicon drift detectors.

Silicon Drift Detector Performance in the SSC Environment

The Monte Carlo of the Silicon Drift Chamber was done within the GEANT framework. Two generators were used, ISAJET and a simple few-particle generator used for cross-checking. The detector modelled is the 8 anode silicon drift detector sized to fit a 4 inch wafer. The area per anode is 1.6cm in the drift direction and 3.2cm in the transverse direction. This detector measures precisely only one coordinate and is equivalent to a microstrip detector but needs much fewer channels. It is a good candidate for layers of the inner tracking detector farther away from the intersection region. (Candidate layers are called a,b and maybe c in Fig. 15.) In this simulation, however, we have placed this large size silicon drift detector into the d–layer, which is only 10cm away from the SSC beams. The reason for placing such a relatively coarse and large detector so close to the beams was to study the possible problems of the detector for a smaller number of generated events.

The Monte Carlo consisted of two parts. The first was a generator and tracking program that found the hits in the detectors, made the digitization and wrote the results to tape. The second was a reading and reconstruction program that read this "data" back. The original hit banks were also included on tape for comparison with the reconstructed results. Two detector layers were modelled simultaneously in all event generations. One detector in a required position, and another parallel detector immediately behind the first. The anode placement was identical in the parallel detector, but with the opposite drift direction to reconstruct the beam crossing time.

The detector performance was modelled using a parameterization of the drift of the charge left by the original ionizing particle. The width of the charge cloud as it drifts has been calculated and compared to measurements, as a function of total charge and total

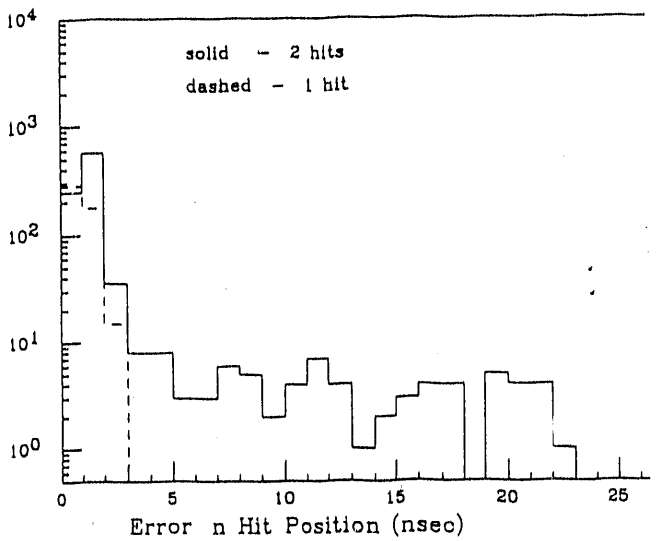

Figure 16: Reconstruction Accuracy for 1 and 2 hits randomly placed within an Anode

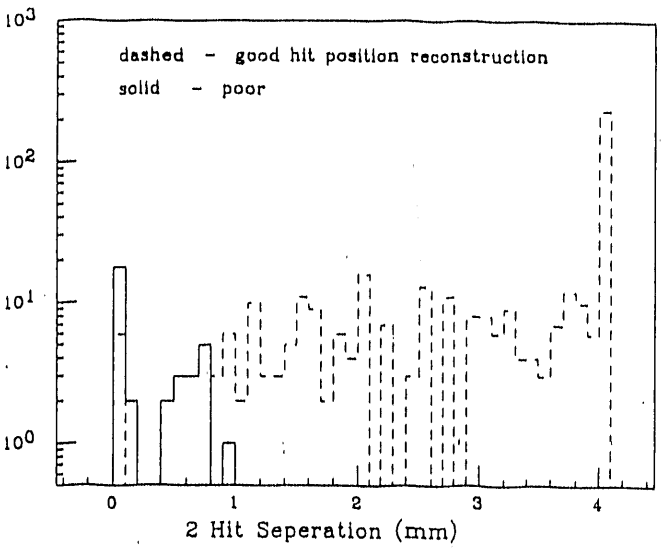

Figure 17: Seperation between the 2 randomly placed hits when the reconstruction error was small, and when it was large.

drift time. This time evolution of the charge cloud accounted for self-repulsion and diffusion. The position of a hit tracked to the detector was then drifted in software towards the anode region. The drift electric field was chosen to be 600 V/cm (for a drift velocity of the charge carriers of $8\mu m/ns$). The software simulated a gaussian shaping amplifier with a shaping sigma of 20 nsec. Due to the diffusion and repulsion of the charge cloud, the typical width of the gaussian signals after the digitization is nearer to 30 nsec.The output of the shaping amplifier was digitized in a fake Flash ADC in 16 nanosecond steps.

The values of the drift field, shaping amplifier time constants and the sampling frequency were taken from the drift detector to be used in the NA-45 experiment at CERN. The parameters of the design were frozen more than a year ago at rather conservative values. We hope to run silicon drift detectors faster at the SSC, which requires a higher value of the drift voltage and a higher bandwidth of the read-out of used electronics. We used the conservative values again to see the problems with the detector.

The reconstruction program would sequentially scan each digitization stored on tape and search for the expected gaussian-shaped response of a hit. The center of the gaussian response was fit using both a simple center of gravity calculation and also a chi-squared minimization with the fitting program MINUIT. The result was compared to the original hit banks. This method was repeatedly applied to a given event, until all signals over a certain threshold were found and subtracted. Some improvement was found over the center of gravity method, when using the MINUIT fitting. It is thought that even this could be improved upon. The method presented here is the simplest, using the center of gravity calculation.

The strategy of the Monte Carlo was to start with the generation of a single particle to compare the digitization for this single hit with that expected. The reconstruction efficiency and accuracy were determined, to judge the method. Two particles were then simulated from the same bunch crossing to judge the interference in reconstructing each position and the bunch crossing time. Two particles, however, from different bunch crossings were then generated.

Fig. 16 shows the error in the reconstruction of a hit. Note carefully that the vertical scale is logarithmic. Each hit has an expected drift time; the difference between this time and the reconstructed drift time is shown here in nanoseconds. A bin of 1 nsec here corresponds to 8 microns. The 2-hit case shows considerable interference in the drift time reconstruction. Fig. 17 shows the spatial separation between the two hits, for two cases. The first case (shown dashed,) is where the drift time reconstruction error in Fig. 16 was less than 5 nsec for both hits. The solid line histogram shows the case when the drift time reconstruction error is greater than 5 nsec.

The drift time reconstruction of the two hits becomes poor when their separation from each other is less than about 1 mm. With the width of the output of the pseudo-gaussian shaper having an average sigma of 30 nsec, 1 mm corresponds to about 4 sigma separation between the two gaussian signals. This is the separation level at which one may expect problems to begin with this simple method. We have published[5] a detailed study of the double particle resolution showing deterioration of the resolution only by a factor of two at 2 sigma separation. It should be stressed

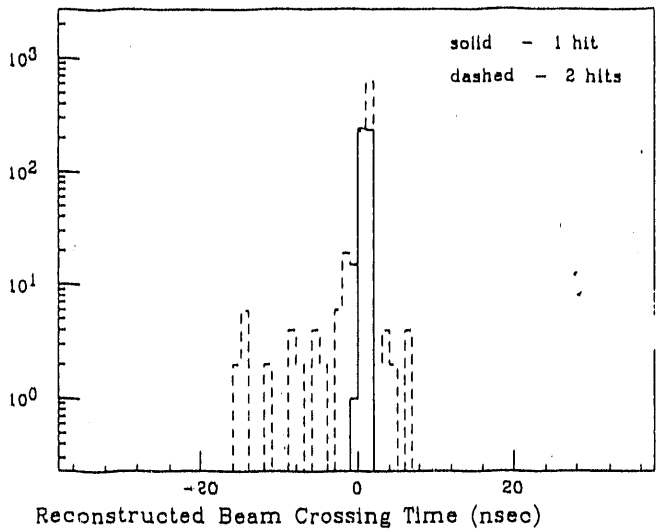

Figure 18: Beam Crossing Time reconstructed from 1 and 2 hits in an anode

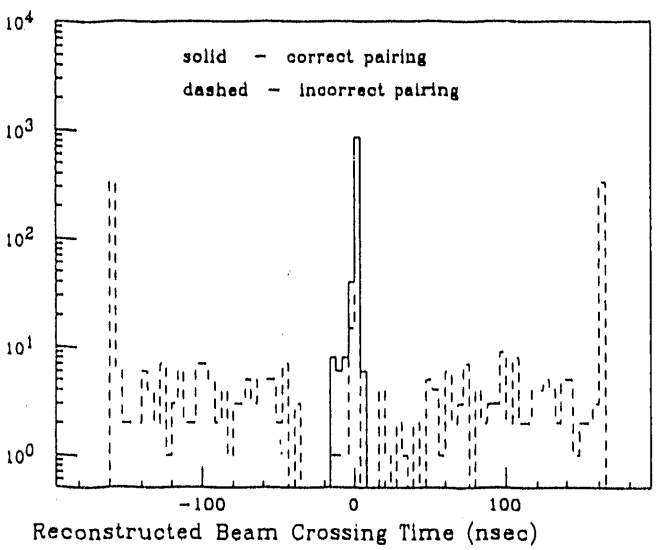

Figure 19: Reconstructed beam crossing time for two hits in two parallel detectors, for correct pairing between the two detectors, and for incorrect pairing.

that a more sophisticated method would be expected to give a smaller separation between neighboring signals before appreciable interference results.

We see that the reconstruction method used up to now in the software simulation is not the optimum one and provides results inferior to the real measurements.

This "interference separation" also affects the beam crossing time reconstruction. Fig. 18 shows the reconstructed beam time crossing, for the case of 1 hit in an anode in the detector and for 2 hits in the same anode. It is expected here that perfect performance would show two sharply peaked curves at 0 nsec. It was found

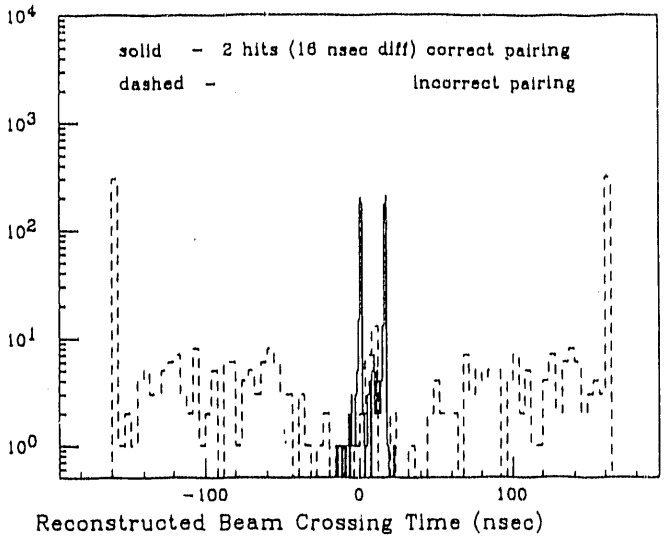

Figure 20: Reconstructed beam crossing time for two hits in two parallel detectors from two consecutive beam crossings, for the correct pairing between the two detectors, and for the incorrect pairing.

that the tails in the 2-hit case occurred when the 2 hits were again within 1mm of each other. Again, it is anticipated that a more sophisticated reconstruction method of separating two nearby hits could be more usefully applied.

Fig. 19 shows the contamination due to incorrect pairing of two hits in two parallel detectors. The solid histogram shows the correct pairing, the random dashed background the incorrect. The peaks near $\pm 160ns$ are underflow and overflow. The central peak is contaminated at a level of several percent. The background due to incorrect pairing shows very weak structure. This will be studied further, to guarantee that incorrect pairing in the reconstruction between the two detectors does not lead to systematic errors in the beam reconstruction time.

Fig. 20 shows the same reconstructed crossing times for two hits, where the hits are separated by 16 nsec. The correct pairings displays the expected time difference.

What has been demonstrated then is that with a simple method, a reasonably accurate reconstruction can be made of 1 and 2 particles in an anode. The failures even with this method are at the level of a few percent.

The Monte Carlo tracking was applied using ISAJET minimum bias events. Table 1 shows the population of each of the detectors nearest the interaction region for one such test. We can see:

- The placement of the detectors corresponds approximately to the same rate in each detector. This is close to the ideal situation.
- Every detector receives about 40 hits over the detector, or an average of 5 hits per anode. This number

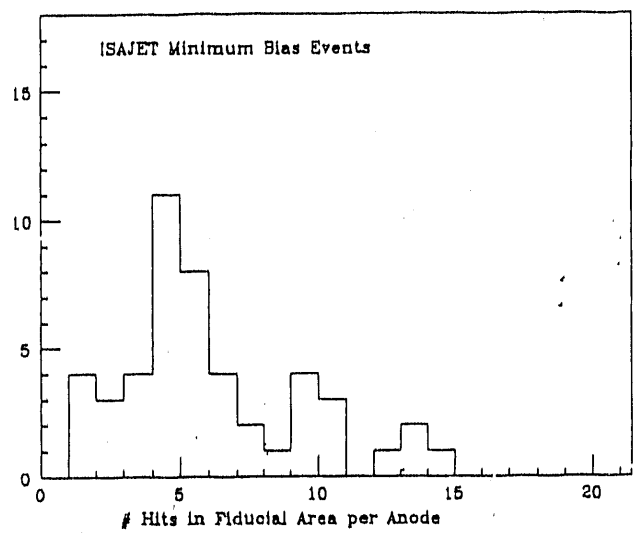

Figure 21: The distribution of the number of hits per anode is shown, for ISAJET minimum bias, in the fiducial area of the detector.

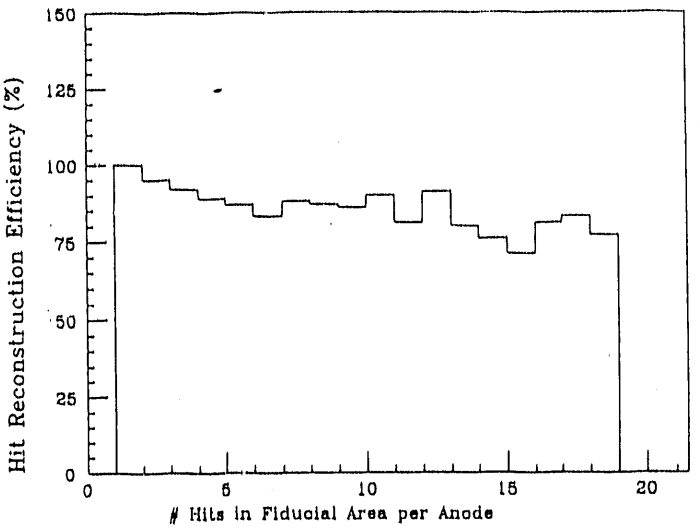

Figure 22: The efficiency for identifying and fitting a hit signal in the presence of other pileup hits is shown. Here the method of identifying a hit uses a center of gravity calculation about a peak, and subtraction according to the known amplitude for a minimum ionizing hit.

Table 1: Hit counts vs. detector position in a $6.4 \times 6.4 cm^2$ detector in $2\mu s$ for minimum bias events at luminosity of $10^{33} cm^2 s^{-1}$

Position	Number of hits
D4	47
D3	45
D2	44
D1	37
D0	40

of hits is only about a factor of two higher than an acceptable number of hits. That means that rather large detector elements of 1.6 cm × 1.6 cm are sufficient for a luminosity of $10^{33} cm^{-2} s^{-1}$ at 10 cm distance from the SSC beams. Fig. 21 shows the hit distribution per anode in this fiducial area accumulated over several Monte Carlo runs. We know from the analysis of the previous subsection that 5 hits accumulated during the memory time of the silicon drift detector are too many. The remaining plots are for now only of academic interest, to show that the performance of the detector deteriorates only slightly with higher occupation numbers. This feature, however, may become important with higher luminosities at the SSC in the future. The ability to reconstruct these hits was examined, and the results are shown in Fig. 22. In the 1-hit case, this efficiency is understandably 100%, dropping off by approximately 5% over each of the next few hits, and reaching a plateau at about 75-80%. To be able to obtain such high multiplicities a special run of two jet event was performed.

Conclusions

- It is possible to monitor and to calibrate out the changes in the drift time in silicon drift detectors with temperature. The calibration is achieved by a simple pulsing of an electrode on the detector.
- The systematics of the silicon drift detector provides a resolution about $10\mu m$ in both directions without the use of a special set of calibration constants. To improve the resolution to $5\mu m$, a special set of detector calibration constants is required.
- There is no problem with the memory time of silicon drift detectors used at the SSC at the luminosity of 10^{33} at a distance of 10 cm from the beams. A pair of drift detectors solves completely the "confusion" problem.

References

1. E. Gatti and P. Rehak, Nucl. Instr. and Meth. 225, 608 (1984).
2. P. Rehak et al., Nucl. Instr. and Meth. A248, 367 (1986).
3. E. Gatti at al.,Nucl. Instr. and Meth. A295, 489-491, (1990).
4. E. Gatti et al.,Nucl. Instr. and Meth. A273, 865-868, (1988).
5. E. Gatti at al., Nucl. Instr. and Meth. A274, 469 (1989).

This research supported in part by the U.S. Dept. of Energy under Contract DE-AC02-76CH00016.

END

DATE FILMED

12/10/90